Sensors & Diagnostics

TUTORIAL REVIEW

View Article Online
View Journal | View Issue

Cite this: *Sens. Diagn.*, 2023, **2**, 320

Biomimetic gold nanomaterials for biosensing, bioimaging and biotherapy: a mini-review

Danzhu Zhu,† Xiaoting Zhang,† Yipeng Han, Xin Luan and Gang Wei *

Gold nanomaterials (AuNMs) have different morphologies, such as nanoparticles (NPs), nanorods (NRs), and nanoclusters (NCs). Due to their unique structures and properties, AuNMs have exhibited broad application prospects in biosensing, bioimaging, and biotherapy. Different from the traditional synthesis methods, biomimetic synthesis can create functional nanomaterials that meet the needs by imitating the internal harmony process or natural structure. Biomimetic synthesis can simplify the synthesis steps and improve the yield of nanomaterials. In this work, we present recent advances in the biomimetic synthesis of various AuNMs, and their potential applications for biosensing of analytes, bioimaging of cells, and the therapy of tumors. In this direction, we first introduce and discuss the studies on the biomimetic synthesis and the properties of AuNMs. Then, case studies on the utilization of AuNMs for the fabrication of biosensors, and the design of functional AuNMs for bioimaging and biotherapy of cancers are carried out. This mini-review will help readers understand the methods of biomimetic synthesis of AuNMs and their potential applications in various fields, while providing new inspirations for optimal design and synthesis of AuNMs with enhanced properties and functions.

Received 13th December 2022,
Accepted 29th January 2023

DOI: 10.1039/d2sd00222a

rsc.li/sensors

College of Chemistry and Chemical Engineering, Qingdao University, Qingdao 266071, China. E-mail: weigroup@qdu.edu.cn, wei@uni-bremen.de; Tel: 0086 15066242101
† Equal contribution to this work.

Gang Wei

Gang Wei received Ph.D. from the Chinese Academy of Sciences in 2007. After his Ph.D. study, he moved to Friedrich-Schiller-University of Jena (Germany) as the Alexander-von-Humboldt and Carl-Zeiss postdoctoral fellow until Dec. 2011. From 2012–2019, he worked as a Senior Researcher and Group Leader at the University of Bremen (Germany). Currently, he is a Full Professor at Qingdao University (China), and the Guest Professor of Ningbo Instutite of Materials Technology and Engineering (CAS). His research interests include 2D nanomaterials, supramolecular self-assembly, biomaterials, and biosensors. Up to now, he has published 190+ papers (Citation > 8800, H-index = 56) in peer-reviewed journals, such as Chem Soc Rev, Prog Mater Sci, Prog Polym Sci, Adv Funct Mater, and others. He is the Associate Editor of the Journal of Nanobiotechnology (BMC Springer), and an Editor Board member of several journals.

1. Introduction

Biomimetic synthesis is a green and environmentally friendly strategy for the preparation of various functional nanomaterials, which can promote the formation of nanomaterials with desired shapes and functions through simulating the unique materials, structures, and functions in natural things.[1] Compared with other chemical and physical synthetic methods, biomimetic synthesis usually does not require redundant ligands, solvents, and reducing/oxidizing agents and can realize the synthesis and applications of nanomaterials under mild conditions with the assistance of biological substances.[2]

Previous studies have indicated that the biomimetic synthesis of metal nanoparticles (NPs) can be realized by some methods, including templated synthesis, seed-mediated synthesis, biomineralization, biometallization, and target anchoring.[3–10] For instance, Ruan *et al.* reported the synthesis of platinum nanoparticles (PtNPs) with peptide templates, which can further be used as nucleation sites for the formation of Pt nanowires at room temperature without the use of additional reagents. The reaction conditions were mild and controllable.[11] In the work of Sheng *et al.*, a gold nanocluster (AuNCs)-anchored manganese dioxide nanomaterial (Au-NCs-MnO_2) was synthesized using bovine serum albumin (BSA) as the biological template,[12] in which the reducing agents and stabilizers were not needed.

Biomimetic synthesized nanomaterials have good biocompatibility and can be captured by biological cells or

targeted to cells. In addition, biomimetic synthesized nanomaterials have the ability to repair and heal biological tissues and organs.[13–17] Compared with other synthetic methods, the mild conditions of the biomimetic synthesis method, the environmentally friendly synthesis method, and the biocompatibility of the synthesized materials make them have high potential in biosensing, bioimaging, biotherapy, and other biomedical applications.

As one type of the widely used metal nanomaterials for various biomedical applications, gold nanomaterials (AuNMs) have good biocompatibility, unique optical properties, and excellent electrical conductivity, revealing wide range of applications in the fields of biosensing, bioimaging, diagnosis, catalysis, and electrochemistry.[18–24] For example, Wang and co-workers constructed a decomposable biomimetic gold nanomaterial (MMV-Au-CDS-DOX) by encapsulating Au-CDs with macrophage-derived vesicles.[25] The biomimetic MMV-Au-CDS-DOX could target tumors to stimulate the tumor microenvironment to be broken into fragments, destroy the growth environment of tumors, and release anti-tumor nanosheets to achieve multimodal therapeutic effects. In another case, Li *et al.* used amino acid-dithiocarbamate as the reducing agent and stabilizer to biomimetically synthesize gold nanoparticles (AuNPs), which exhibited negligible toxicity to liver cells and improved biocompatibility.[26]

Besides that, many studies have proved the successful synthesis of AuNMs through biomimetic methods, which can be potentially utilized for the fabrication of high-performance biosensors for detecting different analytes. In addition, AuNMs can be functionalized with functional biopolymers, biomolecules, and other functional nanoscale building blocks for enhancing their applications in bioimaging and biotherapy. For instance, a hybrid material loaded with polycationic AuNPs was biomimetically synthesized for colorimetric detection of amphetamine-type stimulants.[27] The surface of AuNPs modified with cetyltrimethylammonium bromide (CTAB) had many cations, and the electrostatic interaction with graphene oxide (GO) was achieved through electrostatic interaction to obtain the GO-CTAB-AuNP hybrid nanozyme, which catalyzed amphetamine (AMP) and methamphetamine (MAMP) to decompose and oxidize TMB to produce a blue substance in the presence of hemin achieving the purpose of biosensing to detect AMP and MAMP.

Biomimetic AuNMs with different functional uses can be obtained by adjusting the substances that modify AuNPs. In the work of Cui *et al.*, BSA-coated AuNCs were biomimetically synthesized at room temperature through the protein guidance, which exhibited highly selective targeting of MGC803 cells in folic acid coupling and fluorescence imaging capabilities.[28] The powerful properties of AuNMs themselves can further amplify or strengthen the performance of AuNMs after surface modification, which makes it possible to obtain biomimetic hybrid AuNMs, and realize extended applications in different fields.

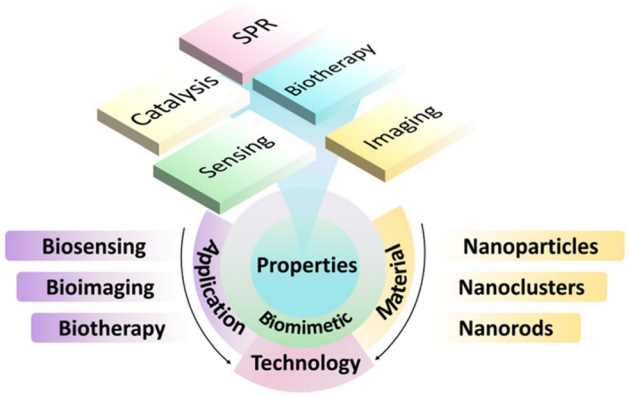

Scheme 1 Schematic diagram of biomimetic synthesis methods, properties, and applications of biosensor, biological imaging and biological therapy of AuNMs.

Although many studies on the biomimetic synthesis of AuNPs, AuNRs, AuNCs, and others for biosensing, bioimaging, and biotherapy have been released,[23,29–31] there are very few reviews to comprehensively elaborate the key parts of biomimetic synthesis, function regulation, and bio-applications of AuNMs. Compared with the previously published articles on biomimetic and biomedical applications of gold nanomaterials, our work describes the various morphologies of gold nanomaterials, the biomimetic synthesis methods of gold nanomaterials, and their applications in biomedical fields. A series of synthesis methods and properties of gold nanomaterials are comprehensively summarized, which have a very wide coverage, with the aim to help readers fully understand the application of biomimetic synthetic gold nanomaterials in the field of biomedicine. Therefore, in this work, we provide a mini-review on the biomimetic synthesis of AuNMs for biomedical applications. The corresponding contents include the biomimetic synthesis method of AuNMs, various properties and functions, and the bio-applications of bioimaging, biosensing and biotherapy. We hope that the introduction and discussion of the biomimetic synthesis, properties, functions, and applications of AuNMs in this work can promote the understanding of design, synthesis, and functional regulation of AuNMs, and further inspire advanced applications of AuNMs (Scheme 1).

2. Synthesis methods of biomimetic AuNMs

2.1 Biomimetic synthesis methods

In recent years, the biomimetic synthesis of nanomaterials has attracted increasingly more attention because of its great advantages. In general, biomimetic synthesis can be carried out by imitating the biological processes that organisms use to produce substances or materials. Abundant available biomass and convenient synthesis routes make the biomimetic synthesis of a bio-template a promising method for large-scale preparation of nanomaterials.

The emulsion droplets formed from polyvinylpyrrolidone and additives were used as templates, and silica nanorods were uniformly directionally grown on fiber materials by hydroxyl localization droplet method.[32] As shown in Fig. 1A, the biomimetic material was constructed with a uniform and dense protruding structure similar to the surface of a lotus leaf. The hydroxyl group on the surface of the fiber is the key to the *in situ* growth of silica nanorods. In addition, isolated silicon nanorods (ISN) and silicon nanorod-modified high silicon fibers (SNSF) were synthesized in the oil–water biphasic reaction system.

Organisms often choose several basic biological processes to form biological unit processes to accomplish specific tasks, such as the biomineralization and biometallization. Biomineralization is the use of pre-assembled supramolecular templates or organic polymerization systems to prepare highly controlled hierarchical and complex structures. Biological macromolecules have complex nanostructures and high-precision molecular recognition ability, which can reasonably control the nucleation process of inorganic nanomaterials. For instance, Ghorbani and co-workers synthesized Bessel-inspired polydopamine (PDA) nanospheres in a deionized water–alcohol mixed solvent at room temperature and atmospheric pressure under alkaline conditions. The PDA sphere is a kind of bioactive NPs, so the enhancement of the mineralization ability in SBF is due to its inherent chemical activation. Zahr *et al.* reported the successful preparation of 22 nm AuNP rings with and without central NPs on the coat protein plate of tobacco mosaic virus.[33] These structures are the first example of the production of nano-rings that is independent of the substrate, and represents the first step in the realization of solution phase or coating-based metamaterials. Lee *et al.* developed a simple method for the preparation of gold nanowires (AuNWs) using the surfactant-mediated biomineralization of a genetically engineered M13 bacteriophage with specific gold-binding peptides.[34] Through the selective interaction between bacteriophage M13 and Au ions in aqueous solution, AuNWs with uniform diameter were synthesized at room temperature.

Other techniques can also be utilized for the biomimetic synthesis of NMs. For instance, Wu *et al.* used microfluidic spinning technology to regenerate rich silk fibroin, and simulated the new humidity drive of natural spider silk.[35] By controlling the dehydration and shearing of silk fibroin, the fiber arrangement and diameter (Fig. 1B) of microfluidic spinning regenerated silk fibers (MRSFs) were successfully designed. In another case, Cui and co-workers realized the functionalization of polystyrene (PS) NPs by PDA for the formation of biomimetic functional nanomaterials.[36] They soaked the coated NPs in SBF to prepare a hybrid structure and synthesized biomimetic HA. In fact, the modification of PS changed its inert behavior to biological activity, and provides the best template for biomineralization. Through the biomineralization and biometallization, various organic–inorganic hybrid nanomaterials can be created effectively in a green way.

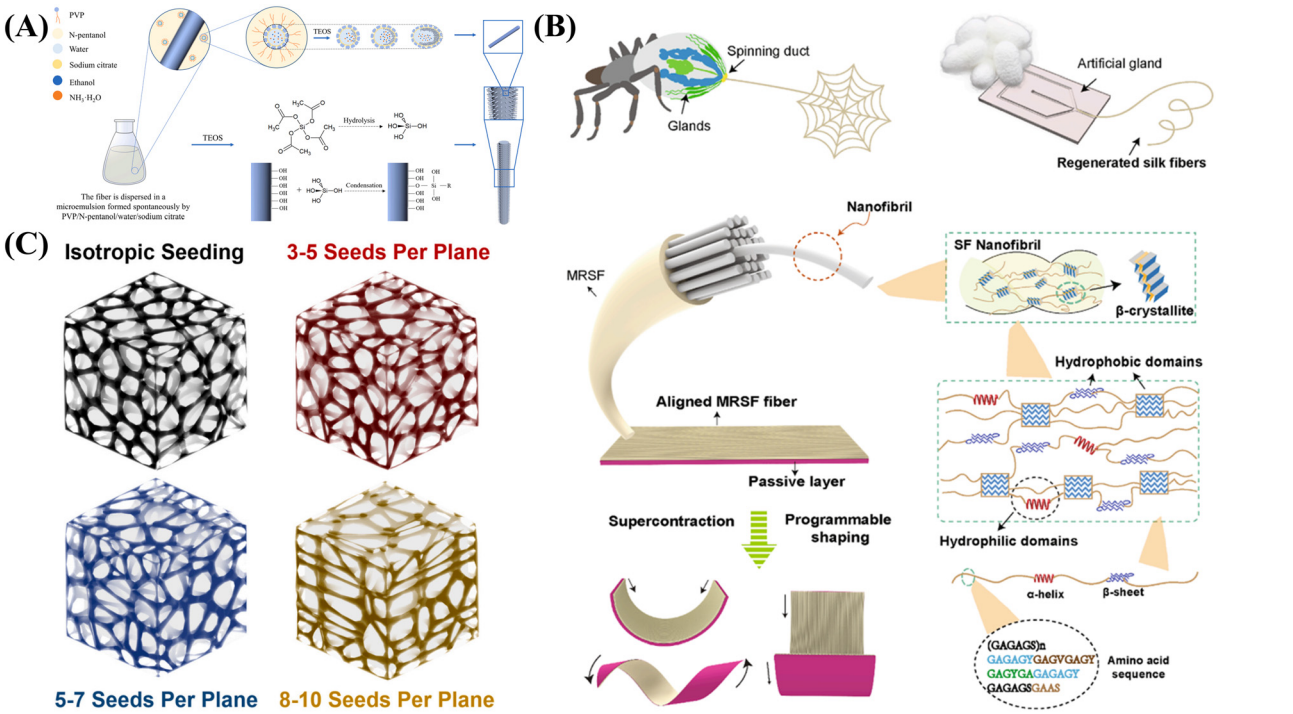

Fig. 1 Biomimetic synthesis of functional nanomaterials: (A) biotemplated synthesis of silica nanorod and SNSF, reprinted with ref. 32 permission from copyright 2022 Elsevier. (B) Concept of mimicking spider silk spinning with microfluidic approach and SF, reprinted with ref. 35 permission from copyright 2022 Elsevier. (C) Biomimetic synthesis of Au-based implants, reprinted with ref. 37 permission from copyright 2021 Elsevier.

By creating a customizable design environment, the selective form of Voronoi mosaic for implant design can better simulate human trabecular bone in terms of anisotropy. In addition, by adjusting the distribution of seeds in the geometric structure of the implant, the implant can design the anisotropic target level that best matches the anatomical structure of the defect,[37] as shown in Fig. 1C. The cubic volume for the selective Voronoi mosaic is a simple implant geometry model, but this technique can also be extended to other more complex implant geometries. This work paves the way for the manufacturing of customizable biomimetic implants.

2.2 Types of biomimetic AuNMs

2.2.1 Au nanoparticles (AuNPs). Many physical and chemical methods, including the top-down and bottom-up techniques, have been developed for the synthesis of AuNPs with adjustable size and functions. The design and synthesis of environmentally friendly AuNPs have attracted great attention because of their low energy consumption, simple process, economy, safety, and non-toxicity.[38] AuNPs have a wide range of applications in biomedicine, optoelectronics, biosensors, and electrochemical catalysis.

A low-cost, simple, environmentally friendly and efficient method to green synthesize AuNPs by reducing gold ions to stable AuNPs using rose aqueous extract has been reported.[39] The prepared AuNPs exhibited antioxidant activity against DPPH (2,2-diphenyl-1-trinitrohydrazine) free radicals and highly catalytic degradation activity against 4-nitrophenol pollutants. These results represent the potential applications of the biomimetic AuNPs in biomedical and industrial applications. Li *et al.* developed a versatile biomimetic nanoplatform (called AuDRM), which has a synergistic effect for photothermal/starvation/immunotherapy for cancer.[40] In the synthesis process, dendritic mesoporous silica NPs were constructed firstly, and then AuNPs were synthesized *in situ* in the mesopores. This paved the way for synergistic photothermal/starvation/immunotherapy with efficient tumor ablation. In another case, the synthesis of spherical high-density lipoprotein (HDL) biomimetics (HDL AuNPs) of different sizes and surface chemistry was achieved using AuNPs as templates, as shown in Fig. 2A.[41]

2.2.2 Au nanoclusters (AuNCs). Metal NCs (less than 2 nm in size) consist of a few to hundreds of noble metal atoms (usually Ag, Au, or Pt), and the spatial limitation of free electrons in metal NCs leads to discrete and tunable electron transitions. This results in molecule-like properties, such as luminescence and unique charging properties. Key

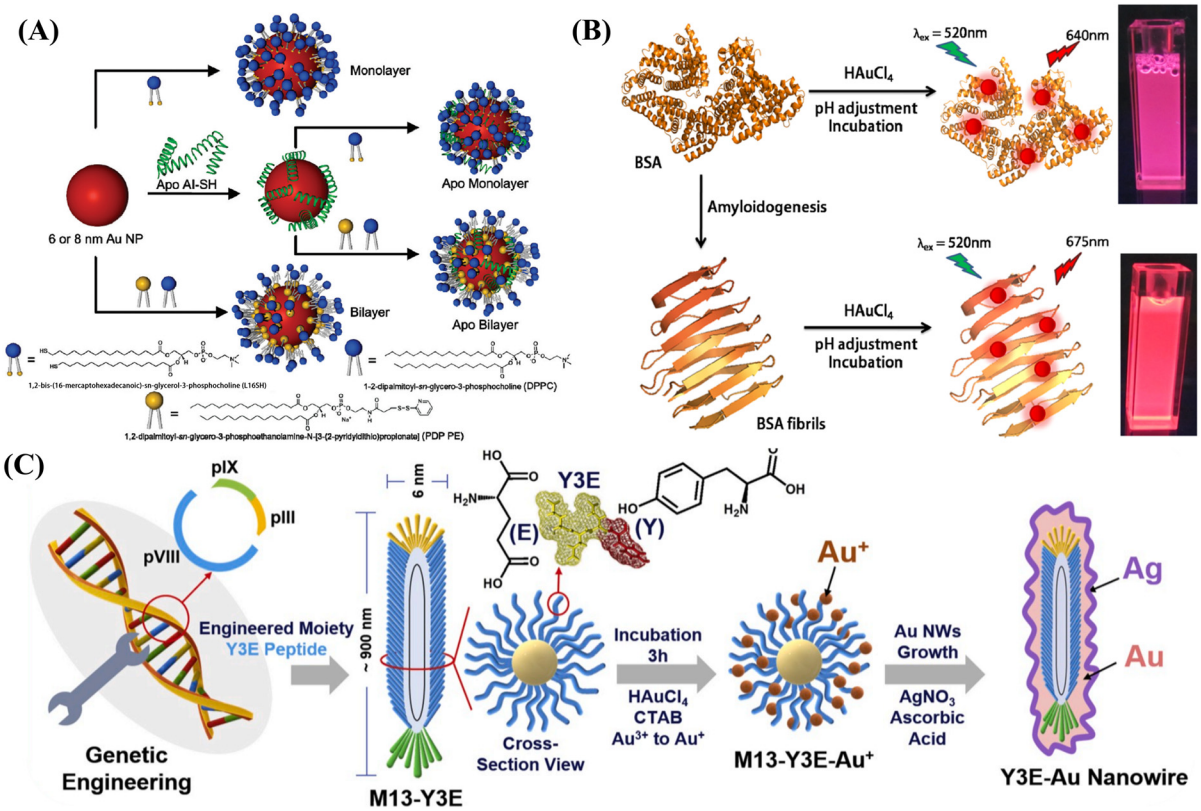

Fig. 2 (A) Biomimetic synthesis of HDL AuNPs, reprinted with ref. 41 permission from copyright 2012 American Chemical Society; (B) biomimetic synthesis of amyloid fiber-functionalized fluorescent AuNCs, reprinted with ref. 46 permission from copyright 2018 American Chemical Society; (C) biomimetic synthesis of gold nanowires using the M13 bacteriophage as a template for colorimetric detection, reprinted with ref. 85 permission from copyright 2020 Elsevier.

characteristics of noble metal NCs allow them to have good fluorescent labeling ability, including high stability under irradiation, large Stokes shifts (good separation of excitation and emission extremes), and magnitude dependence of excitation and emission spectra, which allows the emission values to vary from the visible wavelength region to the near-infrared (NIR) wavelength region, revealing high potential for bioimaging and biotherapy.[42]

Previous studies have indicated that noble metal NCs can be biomimetically synthesized by using various biomolecules such as proteins, peptides, DNA, and small organic molecules as templates, which favor their biocompatibility and make it easy to modify their surface properties for specific applications.[43]

In 2009, fluorescent AuNCs were prepared for the first time using the common sulfate-rich protein, BSA, as the bio-template.[18] The obtained results proved that the formed AuNCs exhibited excellent biosensing and catalytic capabilities. Xie *et al.* developed a new approach using a common protein that can isolate and reduce Au precursors *in situ* to prepare AuNCs with red emission.[44] The formed protein-Au NCs showed unique fluorescence properties, high stability, environmentally friendly synthetic routes, and non-toxic properties, which could be used for the highly sensitive and selective detection of heavy metal ions and biomolecules in food, soil, water, and biological samples.[45] In another case, Nandi and co-workers used self-assembled BSA amyloid nanofibers as bioexcitation scaffolds for the synthesis of Au NCs.[46] As shown in Fig. 2B, amyloid fiber-stabilized AuNCs (FibAuNCs) were created successfully, which revealed significant fluorescence emission enhancement compared to dispersed AuNCs without conjugation with amyloid fibers.

2.2.3 Au nanorods (AuNRs). AuNRs are ideal materials for photothermal therapy (PTT) of tumor cells due to their excellent photothermal transduction effect.[47,48] Red blood cell (RBC) membrane was used as biomimetic coating material to encapsulate AuNRs to enhance their biocompatibility and photothermal stability, and finally achieve a high degree of photothermal ablation of melanoma cells.[49]

Wang *et al.* developed a combinatorial strategy to improve cancer treatment by synthesizing biomimetic albumin-modified AuNRs using paclitaxel (PTX).[50] Li *et al.* described a cell-mediated drug delivery and therapeutic system utilizing macrophage carriers to transport 7 nm diameter AuNRs. Due to their small size, the formed AuNRs exhibited higher macrophage uptake and negligible cytotoxicity compared to AuNRs without protein modification.[51] Jiang *et al.* combined the tumor microenvironment regulation with advanced design of biomimetic AuNRs to propose a new PTT strategy.[52] Biomimetic AuNRs were developed by coating AuNRs with red blood cell membranes. The results showed that cell membrane-modified AuNRs showed significantly higher colloidal stability than pure AuNRs *in vitro*, had a stronger effect on extracorporeal PTT, and revealed a longer circulation time *in vivo*. Meanwhile, the regulation of the tumor microenvironment by cyclopamine successfully disrupted the extracellular matrix of PDA and improved the tumor hemoperfusion.

2.2.4 Au nanocages. The Au nanocage is another kind of gold nano-material with excellent performance. Based on the special cage-like structure of the gold nanocage, it can not only realize the surface loading of other materials, but also embed other materials. Hybrid materials containing gold nanocages can usually achieve targeted drug delivery, PTT, fluorescence imaging and other purposes, which have a broad application prospect in the field of biomedicine.[77–79]

In the work of Liu and team members, the disassembly and self-assembly of apolipoprotein (APO) were realized by adjusting the pH value of the solution, and the DOX was encapsulated in the apolipoprotein nanocage. Then, the Au seeds were added to the solution and grown on the surface of apolipoprotein to form an *in situ* protein nanocage with the Au shell. The cage-like structure formed by the self-assembly of ferritin provides a template for the formation of Au nanocages. The synthesized APODOX-Au has photothermal and anti-inflammatory effects.[80] In the work of Yang and co-workers, a collagenase-functionalized biomimetic drug-loaded gold nano-platform was designed, which combines light-initiated drug release with tumor diagnosis to achieve the effect of targeted drug delivery and treatment *in vivo*. The Au nanocage was synthesized by template method and DOC was loaded into a Au nanocage, and then the extracted pancreatic ductal adenocarcinoma (PDAC) tumor cell membrane was modified into a Au nanocage wrapped in DOX. Finally, collagenase-functionalized Dox-loaded AuNCs (Col-M@AuNCages/Dox) were obtained by lipid insertion coupled with collagenase.[81]

2.2.5 Au nanowires (AuNWs). Metals usually have good electrical conductivity, and metals with linear structure are widely favored because they can enhance the properties of metals in conductivity, catalysis and sensing.[82,83]

In the work of Du *et al.*, Au nanowires were synthesized using flagellar bacteria as templates. The functional groups of flagellar cell proteins can support and participate in the assembly process of AuNWs. The synthesized AuNWs have high electrocatalytic activity and antibacterial activity.[84] In the work of Kim and his team, the biomimetic synthesis of AuNWs using M13 bacteriophage (M13-Y3E) as a template can realize the non-aggregation colorimetric detection of Hg^{2+}.[85] As shown in Fig. 2C, on the template of the M13 bacteriophage, AuNP is determined by the modification of CTAB, and the growth of AuNWs is determined by the connection between bacteriophages. The silver layer on the surface is more favorable for the binding of Hg^{2+} on the surface of AuNWs, thus realizing the colorimetric detection of Hg^{2+}.

To summarize the above introductions and discussion on the biomimetic AuNMs, we present Table 1 to show the details.

Table 1 Materials, biotemplate, structure, and properties of biomimetic AuNMs

Material	Biotemplate	Morphology	Size	Property	Ref.
Au	Eggshell membrane	Nanoparticle	<20 nm	Highly fluorescent	53
Ag	Biotemplating process	Microcoil	—	DC conductivity and self-inductance	54
Ti/Ni	Vessels of vascular plant	Helical structure	11.5–12.5 μm diameter	—	55
Au/Cu, CuO	Diatom	Freestanding structure	—	—	56
TiO_2	Dandelion pollen	Interleaving nanorods	—	Photocatalysis	57
TiO_2	Diatom	Porous	—	Photocatalysis	58
α-Fe_2O_3	Butterfly wings	Quasi-honeycomb	—	Gas sensing	59
Fe_3O_4	Rape pollen	Porous hollow microspheres		Multimodal adhesion	60
Mn_3O_4	Eggshell membrane	Hierarchical network		Water treatment	61
In_2O_3	Cotton fiber	Biomorphic microtubule	30–60 μm length, 8–10 μm width, and 300 nm thickness	Gas sensing	62
SnO_2	Pollen grains	Porous			63
NiO/C	lotus pollen	Hierarchically porous microsphere	35 μm in diameter	Lithium-ion battery electrodes	64
ZnO, NiO, CuO, Co_3O_4, CeO_2	Eggshell membrane	Interwoven microporous structure		Extracting nanoparticles	65
SiO_2	Butterfly wing	Biomorph		Optical property	66
Fe_3C	Leaf	Biomorph		Water splitting	67
Au	Tobacco mosaic virus	Nanoparticle rings	22 nm	Optoelectronic properties	68
Au	M13 virus	Nanowires	10–50 nm	Electrocatalysis	69
TiO_2	Cocci and bacillus	Hollow sphere and hollow tube	micro–nano scale	Hydrogen evolution	70
TiO_2	M13 phage	Nanowires	20–40 nm	Solar cells	71
TiO_2	M13 phage	Network		Solar cells	72
Co_3O_4	M13 virus	Assembled nanowire	*Ca.* 50 nm in diameter and *ca.* 1 um in length	Lithium–oxygen battery	73
V_2O_5	Tobacco mosaic virus	Nanowire	900 nm in length; 100 nm in diameter	lithium-ion battery Electrodes	74
$FePO_4$	M13 phage	Nanoparticles	10–30 nm	Sodium-ion battery	75
$Ca_3(PO_4)_2$	Yeast cell	Hollow microsphere	5–10 μm in diameter		76

2.3 Properties of biomimetic AuNMs

Since the surface functionalization of AuNMs is critical for biological applications, over the past 20 years, there has been a significant amount of research on how to achieve controllable and optimized functional modifications of AuNMs through a large number of building blocks. Until now, various modifiers including small molecules, polymers, and macromolecules have been utilized to modify AuNMs to form stable functional nanomaterials for catalysis,[86,87] biosensing, bioimaging,[88] disease diagnosis, and treatment. In Table 1, we summarize the potential modifiers that can be used to improve the properties and functions of AuNMs for desired applications.

2.3.1 SPR property. The unique surface plasmon resonance (SPR) properties of AuNPs have attracted particular attention in the last years. For the biomimetic AuNPs, the SPR properties are important for supporting their potential applications in various fields. Peptides have been used to modify the surface of AuNPs to control its size, shape, and morphology, which can regulate the SPR properties of AuNPs.[89] Lin *et al.* successfully synthesized BSA-conjugated Au NCs/NPs in water at room temperature by the protein-oriented and liquid-phase green synthesis strategy.[28] The synthesized BSA-Au nanocomposites revealed fluorescence emission at 588 nm of AuNCs and SPR of AuNPs.

Among various AuNMs, AuNRs have attracted increased attention due to their unique SPR band in the NIR region. Due to its unique longitudinal SPR (LSPR) band, AuNRS showed a larger NIR absorption cross-section than other AuNMs (such as the gold nanoshells in clinical trials).[90]

2.3.2 Catalytic activity. Efforts have been made to develop low-cost, high-stable enzyme alternatives. In this regard, nanomaterials with extraordinary enzyme-like catalytic activity (called as nanozymes) are considered suitable candidates. So far, nanozymes have proven to be promising materials for fighting bacteria and biofilms under mild conditions. Emerging studies have proved that various metal and metal oxide NPs, carbon nanomaterials (including carbon nanotubes and GO), and multiple metal–organic frameworks (MOFs) exhibit excellent catalytic activity by mimicking the structure or function of natural enzymes. These nanozyme systems offer higher catalytic stability, ease of modification, and lower manufacturing costs than natural enzymes in a variety of biomedical applications.[51]

Besides the SPR property, AuNMs have high catalytic activity that can be utilized for electrochemical catalysis and biosensors. Luo *et al.* reported an oxidase-like mimic nanozyme based on AuNPs. Although this simulated nanozyme plays a catalytic role, its catalytic products can limit the size and morphology of AuNPs in the form of negative feedback, making them autocatalytic and self-limiting.[51] In order to enhance the catalytic performance of gold nanomaterials, You *et al.* used Amplex UltraRed reagent mediated by hydrogen peroxide, an adenosine analogue in a neutral environment, as the catalytic performance enhancer of AuNMs, modified AuNPs stabilized by sodium citrate with adenosine diphosphate (ADP), enhanced the catalytic activity of AuNPs, and constructed a probe that can be used to detect heparin.[91]

In general, proteins are often used as materials to inhibit catalytic activity. However, in the research of Liu and his team, AuNPs were biomimetically synthesized using polypeptide templates with enhanced catalytic activity, which has good catalytic performance.[92] Also using the template method, Wang *et al.* used cellulose nanocrystals (CNCs) as templates to synthesize AuNPs with adjustable size, which have high catalytic activity.[93]

2.3.3 Sensing property. AuNMs have good stability and sensing characteristics, and can produce a good response under different external stimuli. Their flexibility in retrofitting also makes them potential functional nanomaterials for the construction of various chemical and biological biosensors.[94]

Li *et al.* reported a SiO^{2-} and AuNP-based biosensor, in which the SiO_2 layer acts as a sound wave receiving and guiding device, and stabilizes the receiving antibody. By introducing AuNPs, a competitive immunoassay method was established.[95] Meanwhile, the detection sensitivity of AuNPs to targets was greatly improved after surface modification, indicating that AuNPs are used as a signal amplification actuator.

The obstacles of nanopore modification and characterization limit the development of glass capillary nanopore sensing platforms. To address this problem, Cao *et al.* proposed a simple and effective biomimetic mineralization method to decorate glass nanopores with BSA-protected AuNC (BSA-AuNC) films.[12] The BSA-AuNC membrane emits intense red fluorescence, so it is convenient to make a non-destructive characterization to Au membranes on the inner surface of glass nanopores through fluorescent microscopes.

Sheng and co-workers reported a novel fluorescence/magnetic bimodal sensor based on AuNC-anchored two-dimensional (2D) MnO_2 nanosheets (AuNCs-MnO_2).[96] Using BSA as a template, the formation and assembly of AuNCs-MnO_2 were guided under physiological conditions without the use of strong oxidants, toxic surfactants, and organic solvents. First, the fluorescence of AuNCs is quenched with MnO_2 nanosheets. After the introduction of H_2O_2, MnO_2 nanosheets can be sensitively and selectively reduced to Mn^{2+} while enhancing magnetic resonance (MR) signals and rapidly restoring the AuNC fluorescence. Therefore, a dual-mode detection strategy that overcomes the shortcomings of a single fluorescence detection mode was achieved.

2.3.4 Imaging ability. Fluorescent nanomaterials can serve as important tools for imaging applications. So far, there are a few main types of fluorescent materials, including organic dyes, fluorescent proteins, and nano-probes. Compared to existing organic dyes and fluorescent proteins, Nanoscale Au probes can provide signals that are several times brighter and hundreds of times more stable.[97,98]

For instance, Lin *et al.* successfully synthesized BSA-conjugated AuNCs for bioimaging applications. The BSA-Au nanocomplexes obtained by folic acid molecular coupling have high selectivity and targeting of MGC803 cells, with bimodal darkfield and fluorescence imaging.[53] In the work of Chang *et al.*, the water extract of barley leaves was used to mediate the biomimetic synthesis of AuNPs. In the process of biomimetic synthesis, barley leaf extraction not only plays a role in reducing AuNPs, but also plays a role in stabilizing AuNPs as a capping agent. The synthesized AuNPs had good contrast effects, and exhibited great application potential in clinical CT imaging.[99]

In addition to individual AuNMs, hybrid AuNMs have broad application prospects in radiography and biological imaging. In the work of Tian *et al.*, AuNCs were biomimetically synthesized on the surface of layered hydroxide nano sheets (ELDH) by anchoring. Due to the layered structure, the fluorescence emission of Au in the AuNC/ELDH hybrid material was significantly enhanced, showing excellent imaging performance in cells.[100] By using the fluorescence characteristics of AuNCs, the AuNCs were encapsulated by inhibiting peptidase to prepare fluorescent probes with dynamic nuclear targeting and biosensors, which is an ideal platform for biomedical applications.[101]

2.3.5 Photothermal ability. Nanomaterials with photothermal ability can be injected intravenously or intratumorally, followed by lasering irradiation to raise the temperature to kill tumor cells effectively. In the PTT process, the temperature of tumor tissue lacking blood vessels is 5–8 degrees higher than normal tissue, so cancer cells can be killed first. Different from traditional cancer therapy methods, PTT with biomimetic AuNMs has a few advantages, such as non-invasive, local effect, and few side effects.[54]

Among many gold nanomaterials, the stable and adjustable optical properties of gold nanorods have attracted great attention in photothermal diagnosis and treatment.[102] Zhang *et al.* used this property of gold nanorods to modify the surface of gold nanorods with PEG, which improved the biocompatibility and chemical stability of gold nanorods. Synthetic Au@PEG showed good photothermal effect and biocompatibility both *in vivo* and *in vitro*.[47]

In addition to AuNRs, other morphologies of AuNMs have good photothermal properties. For example, Kang *et al.* investigated the PTT effect of gold nanoshell (AuNS) on the head and neck squamous cell carcinoma (HNSCC) cells.[55]

The analysis of tumor and macrophage mixed models showed that AuNS-based PTT had a strong efficacy under NIR laser irradiation. The *in vivo* toxicological results suggested that AuNS-based photothermal materials may be a promising biocompatible candidate to overcome the limitations of some inorganic photothermal nanomaterials. In the research of Chen and his team, Au nanoweaves were successfully synthesized through the biomimetic synthesis method, combining wet chemistry and layer by layer self-assembly for enhanced tumor imaging and image-guided photothermal diagnosis and treatment. In the process of synthesis, Au nanotears are self-assembled under the guidance of GSH. Au nanotears incubated by GSH have stronger magnetism, and their accumulation in tumors is significantly enhanced, which is more conducive to photothermal diagnosis and treatment.[103] In the work of Shen *et al.*, alginate dialdehyde (ADA) was used as a cross-linking agent to induce the self-assembly of diphenylalanine (FF). At the same time, AuNPs were reduced *in situ* to synthesize ADA-FF/Au nanospheres with high photothermal conversion efficiency, which opened up a road for the application of *in situ* loaded nanoparticles in biomedicine.[104]

3. Biosensing applications

3.1 Colorimetric biosensors

As an important metal material, AuNM has been used in various fields. As a visual detection method, colorimetry has broad application prospects in the rapid detection of many substances. Because AuNMs have different structures and functions, they can show different colors. At the same time, different degrees of aggregation also reveal different colors, making AuNMs suitable candidates for the fabrication of colorimetric sensing platforms without other additional colorimetric agents.[105]

The chemical and physical detection of the causes of diseases are often time-consuming and laborious, and faster, simpler, and more accurate detection methods are needed.[106,107] To achieve this aim, Chen and co-workers synthesized AuNPs with a simple one-pot method using the commonly used antibiotic vancomycin (Van) (Fig. 3A). The vancomycin-coated AuNPs (Van-AuNPs) can selectively interact with Gram-positive bacteria, and can be used to distinguish Gram-positive bacteria from Gram-negative bacteria by naked eye determination. On this basis, a visual colorimetric method of Gram-positive bacteria based on Van-AuNPs was established. Even without any microscopic equipment, the detection limits for Gram-positive *S. aureus*, *M. luteus*, and *B. subtilis* could reach 1×10^9, 1×10^9, and 1×10^9 cells per mL^{-1}, respectively.[108]

In practical biomedical diagnosis, the detection of cancer biomarkers is a necessary basis for cancer diagnosis and treatment. Better testing methods can enable the quick, sensitive, and selective detection of biomarkers. Weng and co-workers synthesized AuNWs by ultrasonic treatment of Au/Bi_2Se_3 precursors and synthetic Au/Bi_2Se_3 nanowires in aqueous solution, which can be used to fabricate an efficient colorimetric biosensor to detect specific cancer biomarkers.[109] The fabricated biosensor had high sensitivity and selectivity towards tumor biomarkers, and the reaction

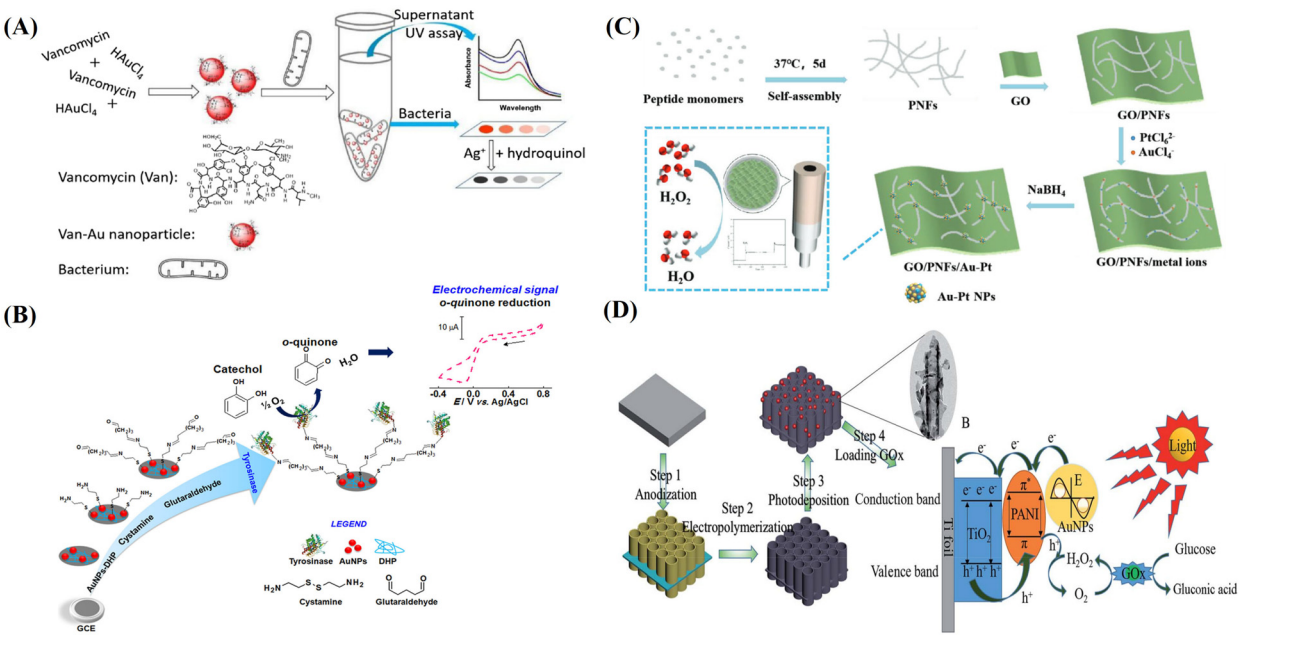

Fig. 3 (A) Biomimetic Van-AuNPs for colorimetric biosensor, reprinted with ref. 108 permission from copyright 2019 Elsevier. (B) AuNPs and DHP-modified GCE for the electrochemical detection of catechol, reprinted with ref. 112 permission from copyright 2016 Elsevier. (C) Biomimetic GO/PNF/Au–Pt nanohybrids for electrochemical H_2O_2 biosensor, reprinted with ref. 113 permission from copyright 2022 Wiley-VCH. (D) Biomimetic synthesis of AuNPs on the PANI-TiONTA electrode for PEC detection of glucose, reprinted with ref. 124 permission from copyright 2020 Royal Society of Chemistry.

concentration for CEA was as low as 160 pg mL^{-1}. In addition, the colorimetric sensor could be used to detect different types of cancer biomarkers, such as α-fetoprotein (AFP) and prostate-specific antigen (PSA).

In addition, because the human body is a compact instrument made up of a variety of biological macromolecules, abnormal concentrations of these molecules are likely to lead to diseases. To deal with this situation, Ilanchelian *et al.* synthesized β-cyclodextrin (β-CD)-functionalized AuNPs (β-CD AuNPs) for the fabrication of a colorimetric sensor.[110] The fabricated colorimetric sensor revealed the rapid and accurate detection of cysteine (Cys). The lowest detection limit of this method for Cys was 25.47×10^{-9} mol dm^{-3}, and the linear detection range for Cys is $2.50–45.00 \times 10^{-7}$ mol dm^{-3}.

3.2 Electrochemical sensors and biosensors

AuNMs have been widely used in the field of electrochemical sensors and biosensors due to their excellent electronic, optical, magnetic, thermal, and catalytic properties.

Peng *et al.* functionalized the exfoliated WS_2 nanosheets with ferrocene monocarboxylic acid (FMC) and AuNPs (AuNPs) by sonochemical method to synthesize ternary AuNP-ferrocene-WS_2 (AFW) composites.[111] At the same time, with the combination of immunomagnetic beads technology and AFW nanocomposites, a high-performance electrochemical immunosensor was successfully developed with carbohydrate antigen (CA72-4) as the model analyte. The fabricated biosensors towards CA72-4 had a linear relationship in the range of 2–50 U L^{-1} with a detection limit of 0.6 U L^{-1}.

In addition, AuNPs have excellent electrical properties and biocompatibility, which are useful for their participation in the development of functional biosensors. For example, Fatibello-Filho used glass carbon electrodes (GCE) that were modified with AuNPs and tyrosinase (Tyr) to construct a biosensor on a 26 alkyl phosphate membrane, as shown in Fig. 3B.[112] The concentration of catechol was determined by the electrochemical amperometric method. The linear range was measured to be from 2.5×10^{-6} to 9.5×10^{-5} mol L^{-1}, and the detection limit was 1.7×10^{-7} mol L^{-1}. Compared with the results obtained by normal spectrophotometry, this method by biomimetic AuNPs had 95% confidence and enhanced sensitivity.

Because AuNMs have the characteristics of simple structure and strong operation, it is easier for small molecules to be adsorbed or coupled to their structures by physical or chemical methods. These characteristics can be well used for the construction of electrochemical biosensors. As shown in Fig. 3C, biomimetic Au–Pt bimetallic NPs were synthesized along self-assembled peptide nanofibers (PNFs) on GO support.[113] PNFs were obtained based on the optimization of experimental conditions, and GO/PNF nanohybrids were formed by non-covalent interaction between PNFs and GO. Due to the biomimetic function of peptide molecules, bimetallic Au–Pt NPs were produced along PNFs through metal ion adsorption and subsequent chemical reduction. The detection limit of the novel electrochemical non-enzymatic biosensor was 0.379 μM towards the detection of H_2O_2, and the linear induction ranges were 1 μM −1 mM and 1–20 mM, respectively.

3.3 SPR biosensors

AuNMs have the characteristics of easy functionalization and tunable optical band, so this material is widely used in research[114–116] for various SPR studies.

In the work of Su and co-workers, AuNPs-enhanced SPR, colloidal gold immunochromatographic strip (ICTS), polymerase chain reaction (PCR), and immunomagnetic separation (IMS) techniques were established for the rapid detection of *Vibrio parahaemolyticus* (VP). The sensitivity of SPR, ICTS, and PCR to VP was 10^1, 10^3, and 10^3 CFU mL^{-1}, respectively. After IMS separation and enrichment, the sensitivities of SPR, ICTS and PCR to VP were 10^0, 10^1, and 10^2 CFU mL^{-1}, respectively, which were 10-, 100-, and 10-fold higher than those of SPR, ICTS, and PCR, respectively.[117]

AuNMs have properties that can be easily modified by various chemicals or biological macromolecules, which were found by El'skaya and his coworkers. An experimental method to improve the sensitivity of the molecular chain based on nucleotides as a carrier of the SPR DNA hybridization sensor was described perfectly. According to the experimental data, the AuNPs modified with specific oligonucleotides could amplify the sensor response of the SPR DNA hybridization sensor about 1200 times.[118]

3.4 Optical biosensors

An optical biosensor is a sensor that converts chemical information into optical information, including photochemical biosensors and fluorescent biosensors. Among them, the photoelectrochemical (PEC) biosensor produces the change of luminous color through electrical excitation, while fluorescence is detected through the quenching of fluorescence by the substance to be detected or the recovery of visible light changes.[119–122] AuNPs have attracted much attention in the preparation of fluorescent biosensors because of their unique optical properties.

For instance, Li and co-workers designed a dual signal amplified electrochemiluminescence (ECL) biosensor for the detection of miRNA-21.[123] The biosensor was based on the isotherm chain replacement polymerase reaction (ISDPR) and bridged DNA-AuNPs nanocomposites. It had excellent uniqueness and high sensitivity, and the detection limit was 3.2 aM with a dynamic range from 0.01 to 10 000 fM.

Because the choice of electrode materials directly affects the ability of the electrode, AuNMs were selected by Wu and his colleagues because of their excellent performance, especially light-trapping ability. A novel PEC sensing platform composed of TiO_2 nanotube array (TiONTAs), polyaniline (PANI), and AuNPs (AuNPs) was successfully constructed, as

shown in Fig. 3D. After loading the enzyme, the Au-PANI-TiONTA electrode showed a good response to glucose in the linear range of 2–36 mM, and the detection limit was 0.02 mM.[124]

As mentioned above, AuNMs can be easily functionalized by various biomolecules and other organic chemicals, and this property is also studied by Li *et al.* In their study, using DNA-functionalized AuNPs (DNA-AuNPs) to initiate the hybrid chain reaction (HCR), a novel label-free electrochemiluminescence (ECL) biosensor was established to detect thymine DNA glycosylase (TDG). Combined with the amplification function of DNA-AuNPs triggered HCR and the inherent high sensitivity of ECL technology, the detection limit for TGD was 1.1×10^{-5} U μL^{-1} (0.0028 ng mL^{-1}).[125]

AuNMs have been selected to fabricate fluorescent biosensors due to their metal-induced fluorescence quenching properties. For example, Jia and colleagues reported the preparation of a novel AuNP probe for 1-cysteine (L-Cys) by biomimetic method, in which the fluorescence resonance energy transfer (FRET) between negatively charged amino capped porous silicon nanoparticles (SiNPs) and positively charged citric acid-stabilized AuNPs were studied.[126] The probe can control the switching of fluorescence. The emergence of this method has opened up a channel for the subsequent development of various NPs.

Functionalized AuNMs usually have good biocatalytic performance, which makes it favored for the fabrication of ECL biosensors. For example, Liu *et al.* reported an ultra-sensitive ECL biosensor for exosomes by using the AuNPs-aptamer (Apt)-modified Ti_3C_2 MXene.[127] Taking full advantage of the large surface area, excellent conductivity, and catalytic effect of the AuNPs-MXene-Apt, the detection limit of the constructed biosensor for the HeLa cell line was 30 cells μL^{-1}, which was more than 1000 times lower than that of traditional ELISA method, and the linear range was 10^2–10^5 cells μL^{-1}.

4. Bioimaging applications

AuNCs have the advantages of good stability, large Stokes shift, good biocompatibility, and easy modification by other biomolecules such as DNA, proteins, and peptides as templates. Therefore, AuNCs and corresponding composites have been widely used in cell targeted imaging and cell metabolism studies.[43]

Zhang *et al.* reported a synthesis method for stabilizing water-soluble fluorescent AuNCs with the double-toothed ligand dihydrolipoic acid (DHLA).[75] Detailed analysis showed that the synthesized AuNCs have ultra-small particle size, good biocompatibility, and high stability, and could be utilized to image the endocytosis process of Hela cells by fluorescence lifetime imaging technology. Tian *et al.* have developed a ratiometric fluorescent biosensor for pH determination, which allows for targeting imagining cancer of cells rich in folate receptor (FR). BSA-protected AuNCs served as the reference fluorophores and fluorescein isothiocyanate (FITC) serves as a response signal for pH detection.[76]

AuNCs are suitable for X-ray imaging due to their high atomic number, electron density, and good X-ray absorption coefficient. AuNCs can also be used as contrast agents for computed tomography (CT) imaging. Wang *et al.* proposed the synthesis of albumin-stabilized AuNCs with red fluorescence and robust X-ray attenuation for bioimaging applications.[128] The *in vivo* studies have shown that AuNCs are distributed in the liver, spleen, and kidneys, and are excreted mainly through the kidneys. Under optimal conditions, the reagent can outline the anatomy of mouse kidneys in 2D and 3D computed tomography and clearly visualize the renal collection system and ureters. This is a promising kidney visualization and disease diagnostic reagent.

In the work of Yan and team members, gold nanoclusters with self-quenching ability were prepared by wrapping AuNCs with BAS, which showed sensitive fluorescence imaging of glutathione *in vivo* and *in vitro*, which is of great significance to the final glutathione *in vivo*.[129] As a common protein, BSA is often used as a crop protective agent. In the work of Yun *et al.*, in order to further stabilize AuNCs and improve their imaging performance, curcumin-coupled AuNCs were synthesized using BSA and curcumin as stabilizers and reducers for fluorescence imaging and anticancer therapy. AuNCs were synthesized by bionic green method without the addition of reducing agents in the whole synthesis process, which also improved the biocompatibility of curcumin and had better anticancer effect.[130]

Wang *et al.* reported a novel simultaneous dual-modal imaging system combining cancer cell membrane-coated NPs as imaging-guided PTT (Fig. 4A).[50] In their study, a new detector capable of simultaneous detection of high-energy X-rays and low-energy visible light was developed based on the cancer cell membrane-coated up-transforming nanoparticles (CC-UCNPs) and AuNPs (CC-AuNPs), which have immune evasion and active tumor targeting capabilities. As shown in Fig. 4B, the biomimetic AuNMs exhibited highly specific bioimaging and highly effective PTT.

It should be noted that highly specific image-guided PTT efficacy could be achieved *in vitro* and *in vivo*. In another study, Gao and colleagues used peptides to recognize AuNPs. The peptide can self-assemble on the surface of AuNCs to biomimetically synthesize the peptide-coupling AuNPs hybrid nanomaterial (HP@AuNPs). As shown in Fig. 4C, after HP@AuNPs enters the cell, it can locate the nucleus and have accurate imaging effectively, which can provide a visual way for the follow-up photothermal diagnosis and treatment.[131]

5. Biotherapy applications

Photothermal therapy (PTT) and photodynamic therapy (PDT) have received considerable attention in the treatment of cancer for many years due to its high therapeutic performance, simple operation, site-specific treatment, and

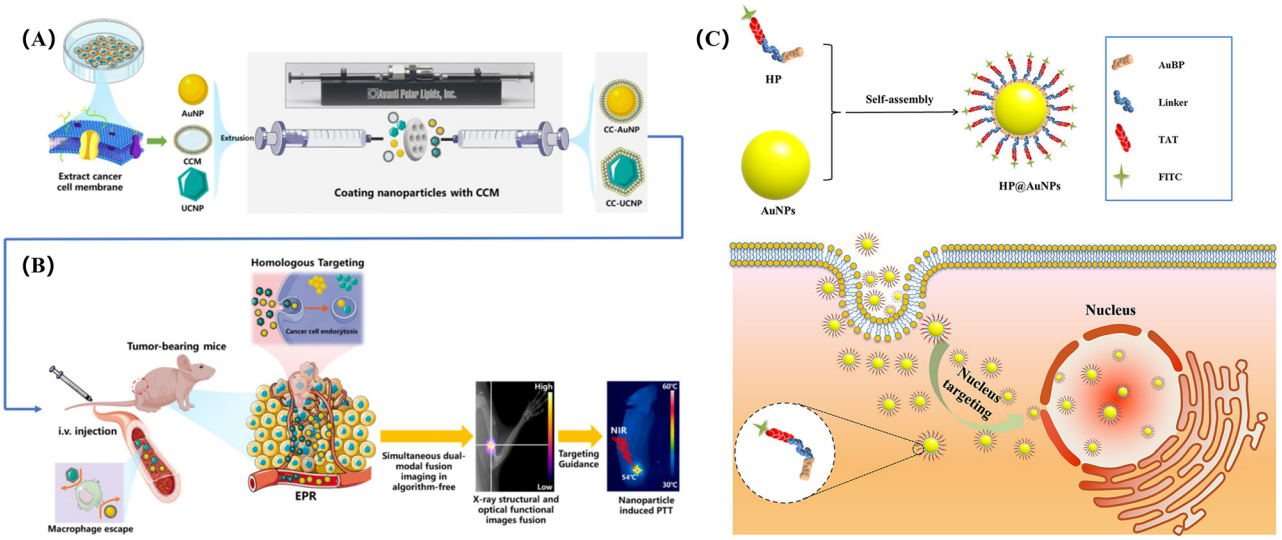

Fig. 4 Biomimetic AuNPs for dual-modal imaging-guided PTT: (A) synthesis procedure of CC-NPs; (B) model for bioimaging and PTT, reprinted with ref. 50 permission from copyright 2020 MDPI, (C) the structure of hybrid peptide-modified AuNPs (HP@AuNPs) and the fluorescence imaging of HP@AuNPs targeting the nucleus of living cells, reprinted with ref. 131 permission from copyright 2020 American Chemical Society.

teleoperation capabilities. For PTT, the light of a specific wavelength irradiates the photothermal agent, causing the photothermal agent to heat and kill tumor cells. As for the PDT, the photosensitizer can generate a large number of reactive oxygen species (ROS), thus showing high efficiency for killing tumor cells.[132] Among the many materials with PTT and PDT capabilities, AuNMs are potential candidates for these applications.

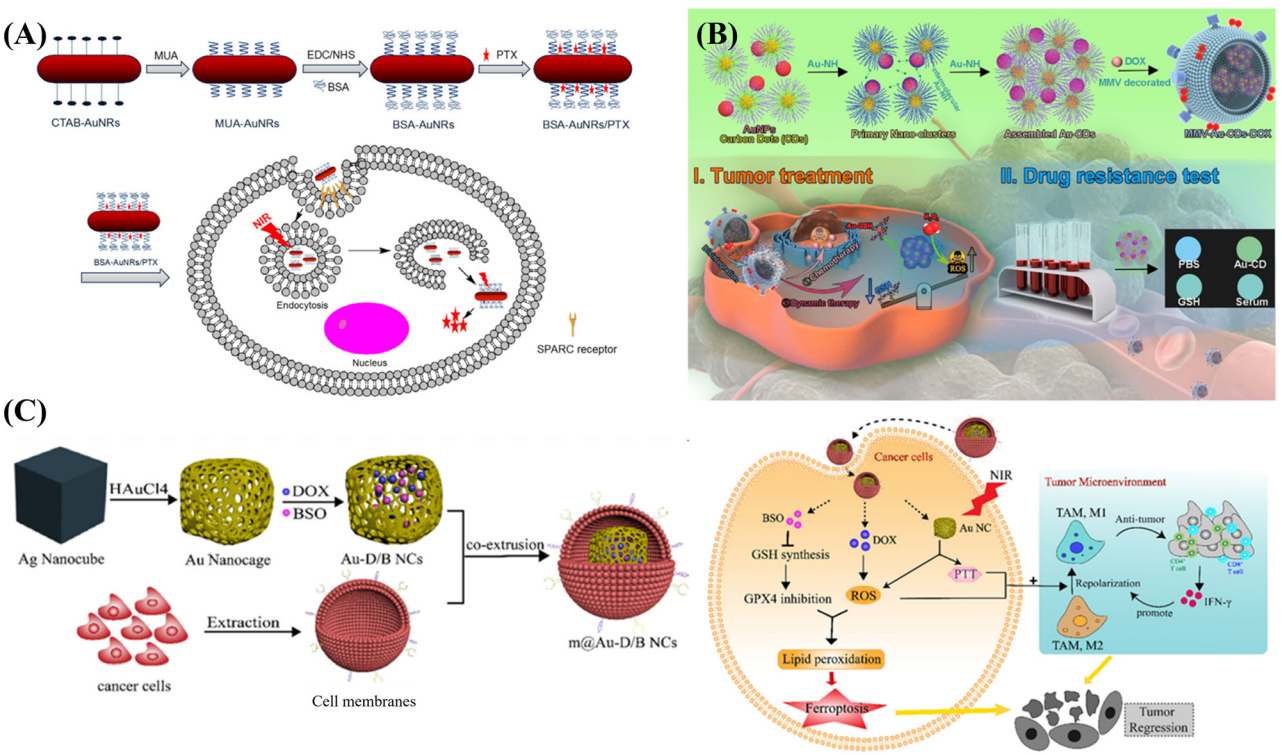

Fig. 5 Biomimetic AuNMs for phototherapy: (A) biomimetic CTAB-AuNR for targeted PTT of tumor cells *in vivo*, reprinted with ref. 96 permission from copyright 2018 Elsevier. (B) MMV-Au-CDs for combined PTT/chemo treatment of tumor, reprinted with ref. 25 permission from copyright 2022 Elsevier. (C) Silver nano-cube as template biomimetic synthesis of gold nano-cage loaded with DOX and BSO to achieve intracellular PDT and PTT synergistic therapy, reprinted with ref. 140 permission from copyright 2022 Elsevier.

5.1 PTT

PTT utilizes the photothermal effect of inorganic NPs to generate heat to kill cells through laser irradiation, which is an anticancer therapy with great application potential. AuNMs have excellent photothermal effect, easy surface modification, and good biocompatibility, making them highly useful for PTT.[133,134]

In the work of Jiang and co-workers, biomimetic AuNRs with photothermal effect were prepared by wrapping erythrocyte membranes (REM) on the surface of AuNRs.[52] The biomimetic AuNRs wrapped by REM revealed better stability and particle circulation. In pancreatic ductal cancer cells with sparse blood vessels, the biomimetic AuNRs promoted the circulation of wrapped AuNRs, which continuously reached pancreatic ductal cancer cells and produced heat to kills cancer cells.

Generally speaking, PTT mainly kills cancer cells instead of healthy cells by direct injection into the tumor site, but the direct injection method will cause the problem of uneven distribution of photothermal materials. Therefore, it is imperative to prepare tumor-targeted photothermal materials for targeted cancer therapy. For example, Li *et al.* prepared CTAB-AuNRs with cations on the surface through a seed-mediated biomimetic synthesis method, which can target tumor cells through further modification, thus realizing high-performance PTT of AuNRs *in vivo*.[96] As shown in Fig. 5A, 11-thiol undecanoic acid (MUA) was modified onto the surface of CTAB-AuNRs through the interaction between sulfhydryl groups and gold. Subsequent activation of the carboxyl group of MUA with EDC and NHS enabled binding to BSA. The loading of paclitaxel (PTX) onto BSA-AuNRs was achieved successfully through the interaction between PTX and protein. BSA in BSA-AuNRs/PTX was an important participant in the metabolism of tumor cell survival, and can be taken up by tumor cells. Therefore, the biomimetic BSA-AuNRs/PTX with photothermal effect realized NIR PTT, and could release anti-tumor drug PTX after being taken up by tumor cells, achieving the effect of dual-mode chemo/photothermal therapy.

In the process of PTT and PDT, the participation of oxygen is essential. However, in actual situations, some tumor environments are often hypoxic environments, which usually limits the performance of hybrid materials in tumor cells. To solve this problem, Yang *et al.* developed a biomimetic AuNP-based hybrid nanozyme that is capable of generating oxygen and generating photothermal effects in a hypoxic environment.[135] In their work, manganese dioxide and ultrasmall AuNPs were deposited onto mesoporous silica nanorods. Manganese dioxide can catalyze H_2O_2 to accelerate oxygen production in hypoxic solid tumors, and AuNPs can catalyze glucose to accelerate thermal ablation of cells.

5.2 PDT

PDT is a non-invasive therapy that can replace chemotherapy and reduce the suffering of patients. Compared with other drug treatments, PDT provides a better direction for solving clinical treatment and other bioengineering.[136,137]

Wang *et al.* proposed and prepared a degradable biomimetic AuNMs, which realized multimodal diagnosis and treatment such as drug release, photodynamic ablation, and destruction of tumor microenvironment.[25] As shown in Fig. 5B, macrophage microvesicles (MMV) were used to wrap Au-CDs aggregates of AuNPs and carbon dots (CDs), then doxorubicin (DOX) was loaded onto the surface of MMV-Au-CDs, and the obtained MMV-Au-CDs-DOX could localize to the inflammatory site of the tumor cells. In the tumor microenvironment, biomimetic MMV-Au-CDs-DOX can be broken into several fragments, in which Au-CDs with photodynamic properties will stimulate the generation of surrounding ROS for cell ablation, while the DOX acts as a chemotherapeutic drug to kill tumor cells to achieve the purpose of multi-modal tumor therapy. In another work, Dutta *et al.* demonstrated the synthesis of biomimetic AuNCs by a green reduction method in the presence of mucin, which can greatly improve the biocompatibility of AuNPs.[138] After the photosensitizer, methylene blue (MB), was modified onto the AuNC-mucin particles, ROS was generated after the light irradiation, which greatly reduced the survival rate of the Hela cells.

5.3 PTT and PDT

In addition to the remarkable photothermal properties of AuNMs, the hybrid materials formed by modifying or combining with other substances can realize dual-mode PDT/PTT treatment, which can obtain higher treatment effect and efficiency.[139]

In the work of Wei and colleagues, a cancer cell membrane-wrapped Au nanocage (m@Au-D/BNCS) loaded with doxorubicin (DOX) and L-buthionine sulfoximine (BSO) was constructed, which revealed dual mode PDT/PTT potential.[140] As shown in Fig. 5C, Au nanocages were biomimetically synthesized by the ion exchange with $HAuCl_4$ using Ag nanocubes as templates. The synthesized Au nanocages with large cavities exhibited good drug loading properties, and could lock both DOX and BSO. Meanwhile, the wrapping of the 4 T1 tumor cell membrane enables it to be easily recognized by tumor cells. After entering the tumor cells, DOX can interfere with tumor DNA replication, and enter mitochondria and generate ROS to achieve PDT. Meanwhile, BSO can block the synthesis of GSH and induce cell apoptosis. In addition, the NIR absorption of Au nanocages produced photothermal effect and photocatalysis to generate heat and ROS, effectively triggering the ablation of tumor cells.

In the work of Chuang *et al.*, the combination of AuNRs and Ce6 was realized by PEG and PEI, and an AuNR-PEG-PEI (APP)-Ce6-loaded adipose stem cell (ADSC) system was proposed.[141] The biomimetic nanomaterials had the ability to target tumors and penetrate tumor spheres. After entering the tumor, AuNRs acted as the photothermal reagents and

Ce6 acted as a photodynamic reagent inside the tumor. The synergistic effects of AuNRs and Ce6 revealed good inhibitory effects on tumor cells without affecting the normal activities and functions of healthy cells.

5.4 Other biotherapy

In the work of Xu *et al.*, gold nanocages were used to encapsulate DOX for anti-cancer treatment. The gold nanocage is wrapped in the cancer cell membrane (CCM), which enables the gold nanocage to easily locate the location of cancer cells. Then, the anticancer drug DOX with high drug-loading efficiency was loaded into the gold nanocage to synthesize DOX@CAuNC by transmembrane ammonium sulfate gradient method. Under the targeted action of CCM, DOX@CAuNC reaches the location of the tumor. A photothermal effect occurs under light irradiation, and DOX is released to realize the anticancer process of PTT and chemotherapy at the same time.[142] In the study of Fang and team members, DOTA-folic acid and HATU-activated bombesin carboxylic acid were connected to form dendrimers and labeled with ^{177}Lu. The gold nanoparticles were successfully biomimetically synthesized by coupling dendritic macromolecules with gold by *in situ* reduction (^{177}-Lu@DenAuNMs–bombesin–folate). It has the ability of radiation diagnosis and treatment for cancer cells, and the optical properties of gold nanomaterials can provide help for the radiotherapy of hybrid materials and further improve the therapeutic effect.[143] In the work of Kumar and team members, the biomimetic AuNPs were stabilized with seaweed extract. The biomimetic gold nanoparticles have good biocompatibility for normal cells and biotoxicity for cancer cells, which directly induce apoptosis of cancer cells without additional energy excitation.[144]

In order to make the above introduction clearer, here we provide Table 2 to summarize various bio-applications of biomimetically functional AuNMs.

6. Conclusion and outlooks

In summary, we summarize the biomimetic synthesis methods of AuNMs, the types of AuNMs, the properties of AuNMs, and the applications of biomimetic synthetic AuNMs in biosensing, bioimaging, and biotherapy. From the above case studies, it is concluded that AuNMs can be synthesized by the template method, biomineralization, biometallization, electrospinning and directional induction. AuNMs with different morphologies, such as AuNPs, AuNRs, AuNCs, Au nanoshells, Au nanocages, and gold nanocars, can be synthesized by the biomimetic strategies. AuNMs with different morphologies are also different in properties and functions, so that it can play a corresponding role in different fields. Meanwhile, the applications of biomimetic AuNMs in the fields of biosensor, biological imaging, biological diagnosis and treatment are introduced and discussed in detail, which can be useful for future bioanalysis, medical diagnosis, and clinical radiography.

Table 2 Bio-applications of biomimetic AuNMs

Applications		AuNMs	Biomedical application	Ref.
Biosensing	Colorimetric biosensors	Van-AuNPs	Gram-positive bacteria detection	108
		AuNWs	Specific cancer biomarkers detection	109
		β-CD AuNPs	Cys detection	110
	Electrochemical sensors and biosensors	AuNP-ferrocene-WS_2	Carbohydrate antigen detection	111
		AuNPs	Sonochemical method	112
		GO/PNF/Au–Pt	Peptide template method	113
	SPR biosensors	AuNPs	*Vibrio parahaemolyticus* detection	117
		AuNPs	SPR DNA hybridization sensor	118
	Optical biosensors	DNA-AuNPs	miRNA-21 detection	123
		Au-PANI-TiONTA	Glucose detection	124
		DNA-AuNPs	Thymine DNA glycosylase detection	125
		AuNPs-MXene-Apt	HeLa cell detection	126
Bioimaging		AuNCs	Fluorescence lifetime imaging for HeLa	75
		BSA-protected AuNCs	Fluorophores and fluorescein isothiocyanate	76
		AuNCs	X-ray imaging	128
		BSA-AuNCs	Fluorescence imaging	129 and 130
		CC-AuNPs	Dual-modal imaging	50
		HP@AuNPs	Imaging and photothermal diagnosis	131
Biotherapy	PTT	REM-AuNRs	Photothermal	52
		BSA-AuNRs/PTX	Dual-mode PTT therapy	96
	PDT	MMV-Au-CDs-DOX	Multi-modal tumor therapy	138
	PTT and PDT synergistic effect	m@Au-D/BNCS	Dual mode PDT/PTT synergistic effect	140
		AuNR-PEG-PEI (APP)-Ce6	Dual mode PDT/PTT synergistic effect	141
	Chemotherapy	DOX@CAuNC	Dual-mode chemo/PTT therapy	142
	Radiotherapy	^{177}Lu@DenAuNMs-bombesin-folate	Dual-mode PTT/radiotherapy	143
	Biotoxicity	AuNPs	Biotoxicity for cancer cells	144

Compared with other synthesis methods, the biomimetic synthesis method has the advantages of green environmental protection, less raw material requirements and simple synthesis method. In the process of biomimetic synthesis, there is usually no need for the addition of additional substances. Each substance in the synthesis process can perform its own function, make the best use of things, and can achieve the effect of "1 + 1 > 2". The hybrid materials synthesized by biomimetic synthesis do not need subsequent complex purification and produce less pollutants, which is an environment-friendly synthesis method. The biomimetic synthesis method can not only improve the overall performance of hybrid materials on the basis of maintaining the characteristics of raw materials, but also solve some defects of the main materials. It is an excellent synthesis method that can maintain and improve the properties of materials to the greatest extent, which has important research significance.

Based on the controllable size, morphology and good compatibility of AuNMs, AuNMs can be easily combined with other materials to achieve the superposition or enhancement of different properties. As a kind of precious metal family, gold material has a high cost. The synthesis of gold nanomaterials by biomimetic synthesis can greatly improve the utilization rate of gold and reduce the waste in the synthesis process. It is an economical, green and environmentally friendly synthesis method for gold nanomaterials. At the same time, the AuNMs synthesized by biomimetic synthesis have higher biocompatibility, reduce the toxicity and damage to organisms, and promote their broad prospects in biomedical and clinical applications. The AuNMs with various morphologies synthesized by biomimetic synthesis method not only have good catalytic, electrochemical and ion resonance properties, but also have good biocompatibility, which need to be studied further for biomedical applications. It is expected that biomimetic AuNMs will have broad application prospects in bioanalysis, cancer early diagnosis, cell imaging, and tumor therapy in the future.

Conflicts of interest

There are no conflicts to declare.

Acknowledgements

The authors thank the financial support from the National Natural Science Foundation of China (No. 51873225), the High-Grade Talents Plan of Qingdao University, and the Taishan Scholars Program of Shandong Province (No. tsqn201909104).

Notes and references

1 G. T. Zan and Q. S. Wu, *Adv. Mater.*, 2016, **28**, 2099–2147.
2 K. G. Gareev, D. S. Grouzdev, V. V. Koziaeva, N. O. Sitkov, H. L. Gao, T. M. Zimina and M. Shevtsov, *Nanomaterials*, 2022, **12**, 2485.
3 W. T. Yang, W. S. Guo, J. Chang and B. B. Zhang, *J. Mater. Chem. B*, 2017, **5**, 401–417.
4 Y. Li, Z. H. Tang, P. N. Prasad, M. R. Knecht and M. T. Swihart, *Nanoscale*, 2014, **6**, 3165–3172.
5 J. B. He, G. Y. Liu, M. D. Jiang, L. H. Xu, F. F. Kong and Z. X. Xu, *Food Agric. Immunol.*, 2020, **31**, 341–351.
6 J. L. Qin, Z. Y. Zhong and J. Ma, *Mater. Sci. Eng., C*, 2016, **62**, 377–383.
7 R. Bilginer and A. A. Yildiz, *Mater. Lett.*, 2020, **276**, 128191.
8 Y. Cui, D. G. Zhang, K. L. Shen, S. Q. Nie, M. Y. Liu, H. Y. Huang, F. J. Deng, N. G. Zhou, X. Y. Zhang and Y. Wei, *J. Environ. Chem. Eng.*, 2020, **8**, 104369.
9 A. Lishchuk, E. Csanyi, B. Darroch, C. Wilson, A. Nabok and G. J. Leggett, *Chem. Sci.*, 2022, **13**, 2405–2417.
10 Y. Wang, W. S. Zhang, C. C. Gong, B. Liu, Y. D. Li, L. C. Wang, Z. A. Su and G. Wei, *Soft Matter*, 2020, **16**, 10029–10045.
11 L. Y. Ruan, E. B. Zhu, Y. Chen, Z. Y. Lin, X. Q. Huang, X. F. Duan and Y. Huang, *Angew. Chem., Int. Ed.*, 2013, **52**, 12577–12581.
12 J. P. Sheng, X. X. Jiang, L. Q. Wang, M. H. Yang and Y. N. Liu, *Anal. Chem.*, 2018, **90**, 2926–2932.
13 H. J. Wang, Y. Liu, R. Q. He, D. L. Xu, J. Zang, N. Weeranoppanant, H. Q. Dong and Y. Y. Li, *Biomater. Sci.*, 2020, **8**, 552–568.
14 K. Jin, Z. M. Luo, B. Zhang and Z. Q. Pang, *Acta Pharm. Sin. B*, 2018, **8**, 23–33.
15 Z. W. Deng, M. H. Li, Y. Hu, Y. He, B. L. Tao, Z. Yuan, R. Wang, M. W. Chen, Z. Luo and K. Y. Cai, *Chem. Eng. J.*, 2021, **420**, 129668.
16 Y. F. Shi, X. Y. Han, S. Pan, Y. H. Wu, Y. H. Jiang, J. H. Lin, Y. H. Chen and H. M. Jin, *Front. Chem.*, 2021, **9**, 724188.
17 Y. Iwasaki, T. Kimura, M. Orisaka, H. Kawasaki, T. Goda and S. Yusa, *Chem. Commun.*, 2014, **50**, 5656–5658.
18 L. Liu, H. Jiang and X. M. Wang, *TrAC, Trends Anal. Chem.*, 2021, **143**, 116376.
19 P. Si, N. Razmi, O. Nur, S. Solanki, C. M. Pandey, R. K. Gupta, B. D. Malhotra, M. Willander and A. de la Zerda, *Nanoscale Adv.*, 2021, **3**, 2679–2698.
20 Y. Zhou, Z. Wang, Y. L. Peng, F. Y. Wang and L. Deng, *J. Biomed. Nanotechnol.*, 2021, **17**, 744–770.
21 R. Ahmad, J. Fu, N. Y. He and S. Li, *J. Nanosci. Nanotechnol.*, 2016, **16**, 67–80.
22 X. C. Qian, X. Zhou, X. Ran, H. C. Ni, Z. Li, Q. Qu, J. Li, G. B. Du and L. Yang, *Biosens. Bioelectron.*, 2019, **130**, 214–224.
23 B. Liu, Y. Wang, Y. Chen, L. Guo and G. Wei, *J. Mater. Chem. B*, 2020, **8**, 10065–10086.
24 S. Li, L. Y. Zhang, Y. Jiang, S. Y. Zhu, X. X. Lv, Z. Q. Duan and H. Wang, *Nanoscale*, 2017, **9**, 16005–16011.
25 F. Wang, Q. H. Yu, J. Li, J. H. Jiang, T. Deng and C. Yu, *Mater. Today Bio*, 2022, **16**, 100359.
26 L. Li, J. B. Liu, X. H. Yang, J. Huang, D. G. He, X. Guo, L. Wan, X. X. He and K. M. Wang, *Nanotechnology*, 2016, **27**, 105603.

27 O. Adegoke, S. Zolotovskaya, A. Abdolvand and N. N. Daeid, *Talanta*, 2020, **216**, 120990.
28 J. Lin, Z. J. Zhou, Z. M. Li, C. L. Zhang, X. S. Wang, K. Wang, G. Gao, P. Huang and D. X. Cui, *Nanoscale Res. Lett.*, 2013, **8**, 170.
29 J. Liu, T. Cui and Y. Ding, *Compos. Commun.*, 2018, **10**, 209–216.
30 R. R. Nasaruddin, T. K. Chen, Q. F. Yao, S. Q. Zang and J. P. Xie, *Coord. Chem. Rev.*, 2021, **426**, 213540.
31 H. Barabadi, H. Vahidi, M. A. Mahjoub, Z. Kosar, K. D. Kamali, K. Ponmurugan, O. Hosseini, M. Rashedi and M. Saravanan, *J. Cluster Sci.*, 2020, **31**, 1173–1184.
32 F. Y. Yan, L. C. Tong, H. Qin, W. M. Guo, J. X. Liu, W. Xie, P. Z. Gao and H. N. Xiao, *Colloids Surf., A*, 2022, **651**, 129705.
33 O. K. Zahr and A. S. Blum, *Nano Lett.*, 2012, **12**, 629–633.
34 Y. J. Lee, J. Kim, D. S. Yun, Y. S. Nam, Y. Shao Horn and A. M. Belcher, *Energy Environ. Sci.*, 2012, **5**, 8328–8334.
35 R. H. Wu, J. Bae, H. Jeon and T. Kim, *Chem. Eng. J.*, 2022, **444**, 136556.
36 J. L. Cui, C. Ma, Z. N. Li, L. Y. Wu, W. Wei, M. Chen, B. Peng and Z. W. Deng, *RSC Adv.*, 2016, **6**, 6747–6755.
37 J. Deering, K. I. Dowling, L. A. DiCecco, G. D. McLean, B. Yu and K. Grandfield, *J. Mech. Behav. Biomed. Mater.*, 2021, **116**, 104361.
38 J. Qiao and L. Qi, *Talanta*, 2021, **223**, 121396.
39 M. Khoshnamvand, S. Ashtiani, C. Huo, S. P. Saeb and J. F. Liu, *J. Mol. Struct.*, 2019, **1179**, 749–755.
40 Z. W. Li and L. Rong, *ACS Appl. Mater. Interfaces*, 2021, **13**, 23469–23480.
41 A. J. Luthi, H. Zhang, D. Kim, D. A. Giljohann, C. A. Mirkin and C. S. Thaxton, *ACS Nano*, 2012, **6**, 276–285.
42 A. Mathew and T. Pradeep, *Part. Part. Syst. Charact.*, 2014, **31**, 1017–1053.
43 Y. Zhang, C. Y. Zhang, C. Xu, X. L. Wang, C. Liu, G. I. N. Waterhouse, Y. L. Wang and H. Z. Yin, *Talanta*, 2019, **200**, 432–442.
44 J. P. Xie, Y. G. Zheng and J. Y. Ying, *J. Am. Chem. Soc.*, 2009, **131**, 888.
45 H. L. Li, W. L. Zhu, A. J. Wan and L. B. Liu, *Analyst*, 2017, **142**, 567–581.
46 I. Nandi, S. Chall, S. Chowdhury, T. Mitra, S. S. Roy and K. Chattopadhyay, *ACS Omega*, 2018, **3**, 7703–7714.
47 L. X. Zhang, S. Chen, R. Ma, L. J. Zhu, T. Yan, G. Alimu, Z. Du, N. Alifu and X. L. Zhang, *ACS Appl. Nano Mater.*, 2021, **4**, 13060–13070.
48 L. Z. Song, X. Zhou, X. G. Dai, R. R. Wang, G. Cheng, N. N. Zhao and F. J. Xu, *NPG Asia Mater.*, 2018, **10**, 509–521.
49 S. H. Li and L. Zhang, *Dalton Trans.*, 2020, **49**, 2645–2651.
50 R. L. Wang, H. Yang, R. X. Fu, Y. Su, X. Lin, X. Y. Jin, W. L. Du, X. H. Shan and G. L. Huang, *Cancers*, 2020, **12**, 3136.
51 Z. B. Li, H. Huang, S. Y. Tang, Y. Li, X. F. Yu, H. Y. Wang, P. H. Li, Z. B. Sun, H. Zhang, C. L. Liu and P. K. Chu, *Biomaterials*, 2016, **74**, 144–154.
52 T. Jiang, B. Zhang, S. Shen, Y. Y. Tuo, Z. M. Luo, Y. Hu, Z. Q. Pang and X. G. Jiang, *ACS Appl. Mater. Interfaces*, 2017, **9**, 31497–31508.
53 P. S. Devi, S. Banerjee, S. R. Chowdhury and G. S. Kumar, *RSC Adv.*, 2012, **2**, 11578–11585.
54 K. Kamata, S. Suzuki, M. Ohtsuka, M. Nakagawa, T. Iyoda and A. Yamada, *Adv. Mater.*, 2011, **23**, 5509.
55 W. Gao, X. M. Peng, A. Pei, C. R. Kane, R. Tam, C. Hennessy and J. Wang, *Nano Lett.*, 2014, **14**, 305–310.
56 Y. N. Fang, J. D. Berrigan, Y. Cai, S. R. Marder and K. H. Sandhage, *J. Mater. Chem.*, 2012, **22**, 1305–1312.
57 S. J. Bao, C. Lei, M. W. Xu, C. J. Cai and D. Z. Jia, *Nanotechnology*, 2012, **23**, 205601.
58 E. Van Eynde, T. Tytgat, M. Smits, S. W. Verbruggen, B. Hauchecorne and S. Lenaerts, *Photochem. Photobiol. Sci.*, 2013, **12**, 690–695.
59 W. H. Peng, C. L. Zhu, S. M. Zhu, F. Yao, Y. Li and D. Zhang, *J. Mater. Sci.*, 2013, **48**, 4336–4344.
60 W. B. Goodwin, I. J. Gomez, Y. N. Fang, J. C. Meredith and K. H. Sandhage, *Chem. Mater.*, 2013, **25**, 4529–4536.
61 R. Mallampati and S. Valiyaveettil, *J. Nanosci. Nanotechnol.*, 2012, **12**, 618–622.
62 P. Song, Q. Wang and Z. X. Yang, *Sens. Actuators, B*, 2012, **168**, 421–428.
63 A. A. Fazil, J. U. Bhanu, A. Amutha, S. Joicy, N. Ponpandian, S. Amirthapandian, B. K. Panigrahi and P. Thangadurai, *Microporous Mesoporous Mater.*, 2015, **212**, 91–99.
64 Y. Xia, W. K. Zhang, Z. Xiao, H. Huang, H. J. Zeng, X. R. Chen, F. Chen, Y. P. Gan and X. Y. Tao, *J. Mater. Chem.*, 2012, **22**, 9209–9215.
65 R. Mallampati and S. Valiyaveettil, *Nanoscale*, 2013, **5**, 3395–3399.
66 Z. W. Han, S. C. Niu, W. Li and L. Q. Ren, *Appl. Phys. Lett.*, 2013, **102**, 233702.
67 Z. Schnepp, W. Yang, M. Antonietti and C. Giordano, *Angew. Chem., Int. Ed.*, 2010, **49**, 6564–6566.
68 H. Zhou, T. X. Fan, J. Ding, D. Zhang and Q. X. Guo, *Opt. Express*, 2012, **20**, A340–A350.
69 H. Ping, H. Xie and Z. Y. Fu, *J. Materiomics*, 2017, **3**, 83–95.
70 P. Y. Chen, R. Ladewski, R. Miller, X. N. Dang, J. F. Qi, F. Liau, A. M. Belcher and P. T. Hammond, *J. Mater. Chem. A*, 2013, **1**, 2217–2224.
71 D. Oh, J. F. Qi, B. H. Han, G. R. Zhang, T. J. Carney, J. Ohmura, Y. Zhang, Y. Shao-Horn and A. M. Belcher, *Nano Lett.*, 2014, **14**, 4837–4845.
72 E. Pomerantseva, K. Gerasopoulos, X. Y. Chen, G. Rubloff and R. Ghodssi, *J. Power Sources*, 2012, **206**, 282–287.
73 M. Moradi, Z. Li, J. F. Qi, W. T. Xing, K. Xiang, Y. M. Chiang and A. M. Belcher, *Nano Lett.*, 2015, **15**, 2917–2921.
74 M. J. Huang and Y. J. Wang, *J. Mater. Chem.*, 2012, **22**, 626–630.
75 L. Shang, N. Azadfar, F. Stockmar, W. Send, V. Trouillet, M. Bruns, D. Gerthsen and G. U. Nienhaus, *Small*, 2011, **7**, 2614–2620.
76 C. Q. Ding and Y. Tian, *Biosens. Bioelectron.*, 2015, **65**, 183–190.
77 Y. X. Liu, T. Liu, L. Tian, L. L. Zhang, L. L. Yao, T. X. Tan, J. Xu, X. H. Han, D. Liu and C. Wang, *Nanoscale*, 2016, **8**, 19075–19085.

78 G. N. Wang, Y. K. Li, J. L. Liu, Y. J. Yuan, Z. L. Shen and X. F. Mei, *Sci. Rep.*, 2017, **7**, 2442.
79 G. N. Wang, W. Gao, X. J. Zhang and X. F. Mei, *Sci. Rep.*, 2016, **6**, 28258.
80 M. Li, D. Wu, Y. Chen, G. Shan and Y. Liu, *Mater. Sci. Eng., C*, 2019, **95**, 11–18.
81 X. Y. Yang, J. G. Zhang, Q. M. Zhou, J. N. Yu, Y. F. Lu, X. J. Wang, J. P. Zhou, X. F. Ding, Y. Z. Du and R. S. Yu, *J. Nanobiotechnol.*, 2022, **20**, 524.
82 T. Chao, Y. Zhang, Y. Hu, X. Zheng, Y. Qu, Q. Xu and X. Hong, *Chem. – Eur. J.*, 2020, **26**, 4019–4024.
83 J. C. Zhang, L. B. Zhong, Y. H. Sun, A. R. Li, J. Huang, F. B. Meng, B. K. Chandran, S. Z. Li, L. Jiang and X. D. Chen, *Adv. Mater.*, 2016, **28**, 3031–3031.
84 R. J. Du, Y. J. Qu, P. X. Qi, X. B. Sun, Y. H. Liu and M. Zhao, *Nanoscale*, 2020, **12**, 5627–5635.
85 S. Manivannan, S. Park, J. Jeong and K. Kim, *Biosens. Bioelectron.*, 2020, **161**, 112237.
86 D. W. Jiang, D. L. Ni, Z. T. Rosenkrans, P. Huang, X. Y. Yan and W. B. Cai, *Chem. Soc. Rev.*, 2019, **48**, 3683–3704.
87 A. Mishra, M. Kumari, S. Pandey, V. Chaudhry, K. C. Gupta and C. S. Nautiyal, *Bioresour. Technol.*, 2014, **166**, 235–242.
88 S. Jiang, K. Y. Win, S. H. Liu, C. P. Teng, Y. G. Zheng and M. Y. Han, *Nanoscale*, 2013, **5**, 3127–3148.
89 Y. Li, W. Li, K. Y. He, P. Li, Y. Huang, Z. Nie and S. Z. Yao, *Nanoscale*, 2016, **8**, 8591–8599.
90 W. J. Luo, C. F. Zhu, S. Su, D. Li, Y. He, Q. Huang and C. H. Fan, *ACS Nano*, 2010, **4**, 7451–7458.
91 J. G. You, Y. T. Wang and W. L. Tseng, *ACS Appl. Mater. Interfaces*, 2018, **10**, 37846–37854.
92 Y. H. Feng, H. J. Wang, J. Zhang, Y. X. Song, M. J. Meng, J. L. Mi, H. B. Yin and L. Liu, *Biomacromolecules*, 2018, **19**, 2432–2442.
93 C. Wang, F. Song, X. L. Wang and Y. Z. Wang, *Int. J. Biol. Macromol.*, 2022, **209**, 464–471.
94 W. S. Zhang, J. D. Xi, Y. C. Zhang, Z. Q. Su and G. Wei, *Arabian J. Chem.*, 2020, **13**, 1406–1414.
95 S. M. Cao, S. S. Ding, Y. Z. Liu, A. W. Zhu and G. Y. Shi, *Anal. Chem.*, 2017, **89**, 7886–7892.
96 D. D. Li, M. Zhang, F. Xu, Y. Z. Chen, B. F. Chen, Y. Chang, H. H. Zhong, H. Y. Jin and Y. Z. Huang, *Acta Pharm. Sin. B*, 2018, **8**, 74–84.
97 S. H. Kang, Y. K. Lee, I. S. Park, I. K. Park, S. M. Hong, S. Y. Kwon, Y. H. Choi, S. J. Madsen, H. Hirschberg and S. J. Hong, *BioMed Res. Int.*, 2020, **2020**, 5869235.
98 W. S. Zhang, D. M. Lin, H. X. Wang, J. F. Li, G. U. Nienhaus, Z. Q. Su, G. Wei and L. Shang, *Bioconjugate Chem.*, 2017, **28**, 2224–2229.
99 N. C. Xue, C. H. Zhou, Z. Y. Chu, L. N. Chen and N. Q. Jia, *Sci. China: Technol. Sci.*, 2021, **64**, 433–440.
100 R. Tian, D. P. Yan, C. Y. Li, S. M. Xu, R. Z. Liang, L. Y. Guo, M. Wei, D. G. Evans and X. Duan, *Nanoscale*, 2016, **8**, 9815–9821.
101 P. Gao, S. Wu, X. Chang, F. N. Liu, T. Zhang, B. J. Wang and K. Q. Zhang, *Bioconjugate Chem.*, 2018, **29**, 4140–4148.
102 L. R. Zheng, B. Y. Zhang, H. S. Chu, P. Cheng, H. Y. Li, K. L. Huang, X. Y. He and W. T. Xu, *Nanotechnology*, 2020, **31**, 485101.
103 Y. J. Liu, Z. Yang, X. L. Huang, G. C. Yu, S. Wang, Z. J. Zhou, Z. Y. Shen, W. P. Fan, Y. Liu, M. Davisson, H. Kalish, G. Niu, Z. H. Nie and X. Y. Chen, *ACS Nano*, 2018, **12**, 8129–8137.
104 K. W. Shen, Y. T. Huang, Q. J. Li, M. Chen and L. M. Wu, *ACS Omega*, 2019, **4**, 18118–18125.
105 D. Z. Zhu, B. Liu and G. Wei, *Biosensors*, 2021, **11**, 259.
106 Y. Li, W. S. Zhang, L. Zhang, J. F. Li, Z. Q. Su and G. Wei, *Adv. Mater. Interfaces*, 2017, **4**, 1600895.
107 L. Wang, Y. J. Sun, Z. Li, A. G. Wu and G. Wei, *Materials*, 2016, **9**, 53.
108 Q. You, X. D. Zhang, F. G. Wu and Y. Chen, *Sens. Actuators, B*, 2019, **281**, 408–414.
109 L. P. Xiao, A. M. Zhu, Q. C. Xu, Y. Chen, J. Xu and J. Weng, *ACS Appl. Mater. Interfaces*, 2017, **9**, 6931–6940.
110 R. Rajamanikandan, A. D. Lakshmi and M. Ilanchelian, *New J. Chem.*, 2020, **44**, 12169–12177.
111 G. L. Hong, R. T. Chen, L. Y. Xu, X. Lu, Z. Q. Yang, G. B. Zhou, L. Li, W. Chen and H. P. Peng, *Anal. Chim. Acta*, 2020, **1099**, 52–59.
112 F. C. Vicentini, L. L. C. Garcia, L. C. S. Figueiredo, B. C. Janegitz and O. Fatibello, *Enzyme Microb. Technol.*, 2016, **84**, 17–23.
113 B. Liu, P. He, H. Kong, D. Z. Zhu and G. Wei, *Macromol. Mater. Eng.*, 2022, **307**, 2100886.
114 Z. X. Zhang, H. Liu, L. Y. Zhai, J. H. Wu and L. Li, *Chem. Phys. Lett.*, 2023, **811**, 140177.
115 X. P. Liu, J. S. Chen, C. J. Mao, H. L. Niu, J. M. Song and B. K. Jin, *Biosens. Bioelectron.*, 2018, **116**, 23–29.
116 L. M. Guo, Z. Li, K. Marcus, S. Navarro, K. Liang, L. Zhou, P. D. Mani, S. J. Florczyk, K. R. Coffey, N. Orlovskaya, Y. H. Sohn and Y. Yang, *ACS Sens.*, 2017, **2**, 621–625.
117 J. Zhou, C. D. Zhang, X. Zhang, C. Y. Lu, T. H. Ming, Y. Li and X. R. Su, *Arch. Microbiol.*, 2020, **202**, 1025–1033.
118 M. Matsishin, A. Rachkov, A. Lopatynskyi, V. Chegel, A. Soldatkin and A. El'skaya, *Nanoscale Res. Lett.*, 2017, **12**, 252.
119 H. Zhang, H. L. Zhang, A. Aldalbahi, X. L. Zuo, C. H. Fan and X. Q. Mi, *Biosens. Bioelectron.*, 2017, **89**, 96–106.
120 M. Belotti, M. M. T. El-Tahawy, L. J. Yu, I. C. Russell, N. Darwish, M. L. Coote, M. Garavelli and S. Ciampi, *Angew. Chem., Int. Ed.*, 2022, **61**, e202209670.
121 R. Nissler, J. Ackermann, C. Ma and S. Kruss, *Anal. Chem.*, 2022, **94**, 9941–9951.
122 W. Huang, G. B. Hu, L. Y. Yao, Y. Yang, W. B. Liang, R. Yuan and D. R. Xiao, *Anal. Chem.*, 2020, **92**, 3380–3387.
123 A. P. Cui, J. W. Zhang, W. Q. Bai, H. P. Sun, L. Bao, F. Ma and Y. Li, *Biosens. Bioelectron.*, 2019, **144**, 111664.
124 B. D. Yan, X. R. Zhao, D. L. Chen, Y. Cao, C. Z. Lv, J. C. Tu, X. H. Wang and Q. Wu, *RSC Adv.*, 2020, **10**, 43985–43993.
125 W. Q. Bai, Y. Y. Wei, Y. C. Zhang, L. Bao and Y. Li, *Anal. Chim. Acta*, 2019, **1061**, 101–109.
126 H. Y. Zhang and Z. H. Jia, *Sensors*, 2017, **17**, 520.

127 H. X. Zhang, Z. H. Wang, F. Wang, Y. M. Zhang, H. Y. Wang and Y. Liu, *Anal. Chem.*, 2020, **92**, 5546–5553.
128 Y. L. Wang, C. Xu, J. Zhai, F. P. Gao, R. Liu, L. Gao, Y. L. Zhao, Z. F. Chai and X. Y. Gao, *Anal. Chem.*, 2015, **87**, 343–345.
129 C. Dai, C. X. Yang and X. P. Yan, *Nano Res.*, 2018, **11**, 2488–2497.
130 S. Govindaraju, A. Rengaraj, R. Arivazhagan, Y.-S. Huh and K. Yun, *Bioconjugate Chem.*, 2018, **29**, 363–370.
131 Y. Y. Gao, Y. L. Liu, R. Yan, J. F. Zhou, H. Dong, X. Hua and P. Wang, *Anal. Chem.*, 2020, **92**, 13595–13603.
132 Y. Q. Shi, D. Z. Zhu, D. J. Wang, B. Liu, X. F. Du, G. Wei and X. Zhou, *Coord. Chem. Rev.*, 2022, **471**, 214725.
133 L. L. Zou, H. Wang, B. He, L. J. Zeng, T. Tan, H. Q. Cao, X. Y. He, Z. W. Zhang, S. R. Guo and Y. P. Li, *Theranostics*, 2016, **6**, 762–772.
134 X. H. Huang, P. K. Jain, I. H. El-Sayed and M. A. El-Sayed, *Lasers Med. Sci.*, 2008, **23**, 217–228.
135 L. F. Yang, C. C. Ren, M. Xu, Y. L. Song, Q. L. Lu, Y. L. Wang, Y. Zhu, X. X. Wang and N. Li, *Nano Res.*, 2020, **13**, 2246–2258.
136 X. S. Li, J. F. Lovell, J. Yoon and X. Y. Chen, *Nat. Rev. Clin. Oncol.*, 2020, **17**, 657–674.
137 S. Monro, K. L. Colon, H. M. Yin, J. Roque, P. Konda, S. Gujar, R. P. Thummel, L. Lilge, C. G. Cameron and S. A. McFarland, *Chem. Rev.*, 2019, **119**, 797–828.
138 D. Dutta, S. K. Sailapu, A. T. Simon, S. S. Ghosh and A. Chattopadhyay, *Langmuir*, 2019, **35**, 10475–10483.
139 Y. J. Hou, X. X. Yang, R. Q. Liu, D. Zhao, C. X. Guo, A. C. Zhu, M. N. Wen, Z. Liu, G. F. Qu and H. X. Meng, *Int. J. Nanomed.*, 2020, **15**, 6827–6838.
140 Y. W. Wei, Z. H. Wang, J. Yang, R. Xu, H. Z. Deng, S. Y. Ma, T. X. Fang, J. Zhang and Q. Shen, *J. Colloid Interface Sci.*, 2022, **606**, 1950–1965.
141 C. C. Chuang, Y. N. Chen, Y. Y. Wang, Y. C. Huang, S. Y. Lin, R. Y. Huang, Y. Y. Jang, C. C. Yang, Y. F. Huang and C. W. Chang, *ACS Appl. Mater. Interfaces*, 2020, **12**, 30021–30030.
142 Q. B. Xu, J. S. Wan, N. N. Bie, X. L. Song, X. Q. Yang, T. Y. Yong, Y. B. Zhao, X. L. Yang and L. Gan, *Theranostics*, 2018, **8**, 5362–5378.
143 Z. Wang, M. H. Ye, D. H. Ma, J. F. Shen and F. Fang, *J. Biomater. Sci., Polym. Ed.*, 2022, **33**, 197–211.
144 S. Jeyarani, N. M. Vinita, P. Puja, S. Senthamilselvi, U. Devan, A. J. Velangani, M. Biruntha, A. Pugazhendhi and P. Kumar, *J. Photochem.*, 2020, **202**, 111715.